Third-order relativistic many-body calculations of energies, transition rates, hyperfine constants, and blackbody radiation shift in ^{171}Yb$^+$

U. I. Safronova[1,2] and M. S. Safronova[3]

[1]*Department of Physics, University of Nevada, Reno, Nevada 89557, USA*

[2]*Institute of Spectroscopy, Russian Academy of Science, Troitsk, 142090 Moscow, Russia*

[3]*Department of Physics and Astronomy, 217 Sharp Lab, University of Delaware, Newark, Delaware 19716, USA*

(Received 27 December 2008; published 27 February 2009)

Relativistic many-body perturbation theory is applied to studying the properties of singly ionized ytterbium, Yb$^+$. Specifically, energies of the [Xe]$4f^{14}ns_{1/2}$, [Xe]$4f^{14}np_j$, and [Xe]$4f^{14}nd_j$ ($n \leq 9$) are calculated through third order. Reduced matrix elements, oscillator strengths, and transition rates are determined for electric-dipole transitions including the 6s, 7s, 8s, 6p, 7p, 5d, and 6d states. Lifetime values are determined for the 6p states. Electric-dipole ($6s_{1/2} - np_j$, $n = 6 - 12$) matrix elements are calculated to obtain the ground-state E1 polarizability. The hyperfine A values are determined for the low-lying levels up to $n = 7$ of ^{171}Yb II. The quadratic Stark effect on hyperfine structure levels of ^{171}Yb II ground state is investigated. The calculated shift for the ($F = 1$, $M = 0$) $\leftrightarrow$ ($F = 0$, $M = 0$) transition is -0.1796 Hz/(kV/cm)^2, in agreement with the previous theoretical result -0.171 ± 0.009. These calculations provide a theoretical benchmark for comparison with experiment and theory.

I. INTRODUCTION

We report results of *ab initio* calculations of excitation energies, lifetimes, hyperfine constants, and polarizabilities in singly ionized ytterbium. These properties of Yb II are of interest for many applications. Recently, manipulation and detection of a trapped Yb$^+$ hyperfine qubit were presented in [1], demonstrating the possibility of using the trapped ytterbium ions as quantum bits for quantum information processing. It was underlined [1] that the ytterbium Yb$^+$ ion is especially attractive because of the strong $^2S_{1/2} \leftrightarrow ^2P_{1/2}$ electronic transition near 369.53 nm that is suitable for use with optical fibers, making schemes that require the coupling of atomic (hyperfine) qubits to photonic (optical) qubits feasible. Frequency shift of hyperfine transitions in Yb$^+$ due to blackbody radiation was recently investigated in [2]. These transitions play key roles in microwave frequency standards. The calculations are used in finding the frequency shifts due to blackbody radiation which are needed for accurate frequency measurements and improvements of the limits on variation in the fine-structure constant α [2]. The study of ^{171}Yb$^+$ single-ion optical frequency standard at 688 THz was recently reported by Tamm *et al.* [3]. Two ^{171}Yb$^+$ single-ion optical frequency standards operating at 688 THz (436 nm) were compared in order to investigate systematic frequency shifts in the subhertz range. A summary of recent results of absolute frequency measurements of the ^{171}Yb$^+$ standard was also given in Ref. [3].

Previously, ytterbium ion has been studied in a number of experimental [4–27] and theoretical [28–35] papers. The beam-foil technique was used by Andersen *et al.* [6] to determine the $4f^{14}6p_{1/2,3/2}$ radiative lifetimes in Yb$^+$ with 10% accuracy (the lifetimes were determined to be 6.9 ± 0.6 ns and 7.2 ± 0.8 ns, respectively) [6]. The laser-induced fluorescence method [14] yielded most accurate values for the $4f^{14}6p_{1/2,3/2}$ radiative lifetimes in Yb$^+$ (8.0 ± 0.2 ns and 6.3 ± 0.3 ns). Beam-laser measurements [23] of the lifetimes of the $4f^{14}6p_{1/2,3/2}$ levels in Yb II were in good agreement

with the previous experiment [14] but show a significant improvement in precision (8.07 ± 0.09 ns and 6.15 ± 0.09 ns). The $4f^{14}7s_{1/2}$ lifetime was measured using the time-resolved laser spectroscopy by Li *et al.* [24]. Radiative lifetimes, measured by time-resolved laser-induced fluorescence spectroscopy, were reported by Biémont *et al.* [26] for the $4f^{14}6d_j$, $4f^{14}7d_j$, and $4f^{14}8s_{1/2}$ states of singly ionized ytterbium. Free Yb$^+$ ions were produced in a laser-induced plasma. The experimental results were compared with Hartree-Fock (HFR) calculations, taking core-polarization effects into account, and a good agreement (within 25%) between theory and experiment was observed for four levels [26]. Lifetime measurements of the $4f^{14}5d_{3/2,5/2}$ metastable states using single ytterbium ions confined in a radio frequency (rf) trap were reported by Yu and Maleki [25]. Authors underlined that the obtained lifetimes for the $4f^{14}5d_{3/2,5/2}$ states, 52.7 ± 2.4 ms and 7.0 ± 0.4 ms, were in good agreement with previously measured values but differ significantly from theoretical estimates. Investigation of the $4f^{14}[6s_{1/2} - 5d_{5/2}]$ clock transition in a single ytterbium ion was previously presented by Taylor *et al.* [21]. A single ion of ^{172}Yb$^+$ was confined in an electrodynamic (Paul) trap. The lifetime of the $4f^{14}5d_{5/2}$ level was found to be 7.02 ± 0.3 ms, which was explained [21] by two decay channels: $4f^{14}[6s_{1/2} - 5d_{5/2}]$ and $4f^{13}6s^2$ $^2F_{7/2} - 4f^{14}5d_{5/2}$. The branching ratio for decay into the $^2F_{7/2}$ level was measured and found to be 0.83 ± 0.03 [21].

Ultrahigh-resolution microwave spectroscopy on trapped ^{171}Yb$^+$ ions was reported by Blatt *et al.* in Refs. [9,10]. The ground-state hyperfine $A(4f^{14}6s_{1/2})$ constant was determined to be 12 642.812 124 2(14) MHz. A laser optical-pumping double-resonance experiment was performed on electrodynamically confined ^{171}Yb$^+$ ions [9]. The hyperfine coupling coefficient for the ^{171}Yb$^+$ state was investigated by Doppler-free saturated absorption laser spectroscopy in an unenriched Yb hollow-cathode discharge. The value of $A(4f^{14}6p_{3/2})$ constant was found to be 877(20) MHz. Hyperfine structure in

the 369.4 nm $4f^{14}[6s-6p_{1/2}]$ resonance line of the single-valence-electron system Yb$^+$ had been determined by Martensson-Pendrill *et al.* [16] with an accuracy of about 1 MHz by Doppler-free saturated absorption spectroscopy in a sputtered vapor. The values of $A(4f^{14}6s_{1/2})$ and $A(4f^{14}6p_{1/2})$ constants in ^{171}Yb$^+$ ions were found to be 12 645(2) and 2104.9(1.3) MHz, respectively [16].

The relativistic model potential (RMP) approach was used in [28] to calculate atomic properties in Yb II. The influence of polarization of the core by valence electrons on ionization energies and transition probabilities has been studied. Oscillator strengths and lifetimes in Yb II were evaluated by Fawcett and Wilson [29]. Weighted oscillator strengths were tabulated for 2745 spectral lines in Yb II. They belong to transitions between the $4f^{14}6s$, $4f^{14}7s$, $4f^{14}8s$, $4f^{14}5d$, $4f^{14}6d$, $4f^{14}7d$, $4f^{13}6s6p$, and $4f^{13}5d6p$ even configurations, and the $4f^{14}6p$, $4f^{14}7p$, $4f^{13}6s^2$, $4f^{13}5d6s$, and $4f^{13}5d^2$ odd configurations. The calculations included configuration interactions between all configurations of the same parity of the above set. In this work [29], Slater integrals were first computed *ab initio* using a pseudorelativistic Hartree-Fock method and subsequently adjusted by means of a least-squares optimization routine which minimizes the discrepancies between observed and computed levels [29]. Oscillator strengths and lifetime values in Yb II were presented by Biémont *et al.* [32]. These properties were calculated within the framework of a pseudorelativistic HFR approximation combined with a least-squares fitting of the calculated eigenvalues to the observed energy levels. A considerable amount of configuration interaction together with core-polarization effects has been included in the calculations. The quality of the HFR results has been assessed through a comparison with data obtained using the completely independent relativistic quantum-defect orbital (RQDO) method [32]. Relativistic coupled-cluster method (CCM) was applied recently by Nayak and Chaudhuria [35] to compute the low-lying excited states of ytterbium ion. The energies were given for the $4f^{14}5d_j$ and $4f^{14}6p_j$ states, magnetic-dipole (A) constants were obtained for the $4f^{14}6s_j$ and $4f^{14}6p_j$ states, and dipole matrix elements were presented for two $s-p$ transitions [35].

In present paper, we calculate atomic properties of singly ionized ytterbium. First-, second-, and third-order Coulomb energies, and first- and second-order Coulomb-Breit energies are calculated. Reduced matrix elements, oscillator strengths, and transition rates are determined for levels up to $ns=6-8$, $np=6-7$, and $nd=5-6$. Electric-dipole ($6s_{1/2}-np_j$, $n=6-26$) matrix elements are calculated to obtain the ground-state E1 polarizabilities. We investigate the hyperfine structure in ^{171}Yb II. The hyperfine A values are determined for the first low-lying levels up to $n=7$. The quadratic Stark effect on hyperfine structure levels of ^{171}Yb II ground state is investigated. The calculated shift for the $(F=1, M=0) \leftrightarrow (F=0, M=0)$ transition is -0.1796 Hz/(kV/cm)^2, in agreement with previous theoretical result -0.171 ± 0.009 Hz/(kV/cm)^2.

II. CALCULATIONS OF ENERGIES

Results of our third-order calculation of energies, which was carried out following the pattern described in [37–40],

are summarized in Table I, where we list the lowest-order Dirac-Fock energies $E^{(0)}$, first-order Breit energies $B^{(1)}$, second-order Coulomb $E^{(2)}$ and Breit $B^{(2)}$ energies, third-order Coulomb energies $E^{(3)}$, single-particle Lamb shift corrections E_{LS}, and the sum of the above E_{tot}. The first-order Breit energies $B^{(1)}$ include corrections for "frequency dependence," whereas second-order Breit energies are evaluated using the static Breit operator. The Lamb shift E_{LS} is approximated as the sum of the one-electron self-energy and the first-order vacuum-polarization energy. The vacuum-polarization contribution is calculated from the Uehling potential using the results of Fullerton and Rinker [41]. The self-energy contribution is estimated for s, $p_{1/2}$, and $p_{3/2}$ orbitals by interpolating among the values obtained in [42–44] using Coulomb wave functions. For this purpose, an effective nuclear charge Z_{eff} is obtained by finding the value of Z_{eff} required to give a Coulomb orbital with the same average $\langle r \rangle$ as the Dirac-Hartree-Fock (DHF) orbital. The accuracy of this approach was recently investigated in Ref. [45] by comparing the values calculated with this approach with the *ab initio* results of Blundell [46] and Chen *et al.* [47] for Cu-like ions. It was shown [45] that the phenomenological one-electron QED values differ from results of the sophisticated *ab initio* calculation from Refs. [46,47] by about 2%. Since the Lamb shift contribution is small in our calculations, the accuracy of our approach is sufficient.

We find that correlation corrections to energies in Yb$^+$ are large, especially for the 6s and 5d states. For example, $E^{(2)}$ is 9% of $E^{(0)}$, and $E^{(3)}$ is 12% of $E^{(2)}$ for the $6s_{1/2}$ state. These ratios decrease for the other (less penetrating) states. Despite the slow convergence of the perturbation expansion, the 6s energy from the present second-order ($\delta E^{(2)}$) and third-order relativistic many-body perturbation theory (RMBPT) ($\delta E^{(3)}$) calculations is within 0.9% and 0.1% of NIST data [36], respectively.

Below, we describe a few numerical details of the calculation of Yb$^+$. We use B-spline methods [48] to generate a complete set of basis Dirac-Fock (DF) wave functions for use in the evaluation of RMBPT expressions. We use 70 splines of order $k=9$ for each angular momentum. The basis orbitals are constrained to a cavity of radius of 200 a.u. The cavity radius is large enough to accommodate all nl_j orbitals considered here and small enough that 70 splines can approximate inner-shell DF wave functions with good precision. We use 65 out of 70 basis orbitals for each partial wave in our third-order energy calculations since contribution of the ten highest-energy orbitals is negligible. The second-order calculation includes partial waves up to $l_{max}=8$ and is extrapolated to account for contributions from higher partial waves. A lower number of partial waves, $l_{max}=6$, is used in the third-order calculation. We find that the contribution to the third-order energy from states with $l>6$ is no more than 10 and 20 cm^{-1} for 6s and $5d_{3/2}$ states, respectively.

III. ELECTRIC-DIPOLE MATRIX ELEMENTS, TRANSITION RATES, AND LIFETIMES IN Yb II ION

A. Electric-dipole matrix elements

The calculation of the transition matrix elements provides another test of the quality of atomic-structure calculations

TABLE I. Zeroth-order Dirac-Fock (DF), second-, and third-order Coulomb correlation energies $E^{(n)}$, first-order Breit and second-order Coulomb-Breit corrections $B^{(n)}$, and Lamb shift E_{LS} contributions to the energies of Yb II. The total energies $E_{\mathrm{tot}}^{(3)}$ for Yb II are compared with experimental energies E_{NIST} [36]; $\delta E^{(n)} = E_{\mathrm{tot}}^{(n)} - E_{\mathrm{NIST}}$. Units: cm^{-1}.

nlj	$E^{(0)}$	$E^{(2)}$	$E^{(3)}$	$B^{(1)}$	$B^{(2)}$	E_{LS}	$E_{\mathrm{tot}}^{(2)}$	$E_{\mathrm{tot}}^{(3)}$	E_{NIST}	$\delta E^{(2)}$	$\delta E^{(3)}$
$6s_{1/2}$	−90789	−8288	1016	128	−259	18	−99190	−98174	−98269	−921	95
$5d_{3/2}$	−66517	−9003	−1027	156	−546	0	−75909	−76936	−75308	−601	−1628
$5d_{5/2}$	−66037	−8001	−1301	114	−499	0	−74424	−75725	−73936	−487	−1788
$6p_{1/2}$	−66087	−4344	335	91	−120	−1	−70460	−70126	−71207	747	1082
$6p_{3/2}$	−63276	−3606	166	63	−110	0	−66929	−66763	−67877	948	1114
$6d_{3/2}$	−34217	−1989	−249	42	−135	0	−36300	−36549	−36095	−205	−454
$6d_{5/2}$	−33959	−1802	−300	31	−125	0	−35855	−36155	−35710	−145	−445
$7s_{1/2}$	−42008	−2168	246	39	−75	2	−44211	−43965	−43965	−246	0
$7p_{1/2}$	−33604	−1400	67	34	−44	0	−35014	−34947	−34563	−451	−384
$7p_{3/2}$	−32565	−1201	21	24	−41	0	−33783	−33761	−32675	−1108	−1087
$7d_{3/2}$	−20844	−834	−249	18	−57	0	−21717	−21966	−21752	35	−214
$7d_{5/2}$	−20714	−764	−118	14	−54	0	−21518	−21636	−21593	75	−43
$8s_{1/2}$	−24373	−907	100	17	−33	0	−25295	−25195	−25229	−66	34
$8p_{1/2}$	−20494	−646	23	16	−21	0	−21145	−21121			
$8p_{3/2}$	−19993	−562	4	11	−20	0	−20564	−20560			
$8d_{3/2}$	−14033	−438	−48	10	−30	0	−14492	−14540	−14429	−62	−111
$8d_{5/2}$	−13959	−404	−59	7	−28	0	−14384	−14443	−14253	−131	−190
$9s_{1/2}$	−15932	−468	51	9	−17	0	−16408	−16357			
$9p_{1/2}$	−13824	−354	11	9	−12	0	−14181	−14170			
$9p_{3/2}$	−13545	−310	0	6	−11	0	−13860	−13860			
$9d_{3/2}$	−10092	−261	−28	6	−18	0	−10365	−10392	−10464	100	72
$9d_{5/2}$	−10046	−241	−34	4	−17	0	−10300	−10334	−10288	−12	−46

and another measure of the size of correlation corrections. Reduced electric-dipole matrix elements between low-lying states of Yb II calculated in various approximations are presented in Table II.

Our calculations of the reduced matrix elements in the lowest, second, and third orders were carried out following the pattern described in Refs. [49,50]. The lowest-order DF values for transitions between valence v and w states (labeled as $Z_{vw}^{(\mathrm{DF})}$) are given in the third column of Table II. The values $Z_{vw}^{(\mathrm{DF}+2)}$ are obtained as the sum of the second-order correlation correction $Z_{vw}^{(2)}$ and the DF matrix elements $Z_{vw}^{(\mathrm{DF})}$. It should be noted that the second-order Breit corrections $B_{vw}^{(2)}$ are rather small in comparison with the second-order Coulomb corrections $Z_{vw}^{(2)}$ (the ratio of $B_{vw}^{(2)}$ to $Z_{vw}^{(2)}$ is about 1%–3%).

The third-order matrix elements $Z_{vw}^{(\mathrm{DF}+2+3)}$ include the DF values, the second-order $Z_{vw}^{(2)}$ results, and the third-order $Z_{vw}^{(3)}$ correlation correction. It should be noted that the third-order matrix elements $Z_{vw}^{(\mathrm{DF}+2+3)}$ are divided in the following way:

$$Z_{vw}^{(\mathrm{DF}+2+3)} = Z_{vw}^{(\mathrm{DF})} + Z_{vw}^{(\mathrm{RPA})} + Z_{vw}^{(\mathrm{BO})} + Z_{vw}^{(\mathrm{SR})} + Z_{vw}^{(\mathrm{NORM})}. \quad (1)$$

We include the corresponding set of the high-order contributions using the well-known random-phase approximation (RPA) in $Z^{(\mathrm{RPA})}$ term using the procedure described in Ref. [49]. The subscript BO stands for Brueckner orbitals. The last two terms in Eq. (1) describe structural radiation, $Z_{vw}^{(\mathrm{SR})}$, and normalization, $Z_{vw}^{(\mathrm{NORM})}$, terms.

The terms $Z_{vw}^{(\mathrm{RPA})}$ and $Z_{vw}^{(\mathrm{BO})}$ give the largest contributions to $Z_{vw}^{(\mathrm{DF}+2+3)}$. The sum of terms $Z_{vw}^{(\mathrm{RPA})}$ and $Z_{vw}^{(\mathrm{BO})}$ is about 20% of the $Z_{vw}^{(\mathrm{DF})}$ term and has a different sign for the $6s$–$6p$ and $5d$–$6p$ transitions. The value of $Z_{vw}^{(\mathrm{BO})}$ becomes the largest contribution for the $5d$–$7p$ transitions and decreases the value of $Z_{vw}^{(\mathrm{DF}+2+3)}$ by a factor of 2 in comparison with the $Z_{vw}^{(\mathrm{DF})}$ term. The value of $Z_{vw}^{(\mathrm{RPA})}$ becomes the largest contribution for the $6s$–$7p$ transitions and decreases the value of $Z^{(\mathrm{DF}+2+3)}$ by a factor of 2 in comparison with the $Z^{(\mathrm{DF})}$ term. The value of $Z_{vw}^{(\mathrm{DF}+2+3)}$ has a different sign for the $6s$–$7p_{1/2}$ transition in comparison with the $Z_{vw}^{(\mathrm{DF})}$ term. Different sign of the $Z_{vw}^{(\mathrm{DF}+2+3)}$ and $Z_{vw}^{(\mathrm{DF})}$ terms is found also for the $5d_{3/2}$–$7p_{3/2}$ and $5d_{5/2}$–$7p_{3/2}$ transitions (see Table II). The structural radiation $Z_{vw}^{(\mathrm{SR})}$ and normalization $Z_{vw}^{(\mathrm{NORM})}$ terms are small. All results given in Table II are obtained using length form of the matrix elements.

B. Form-independent third-order transition amplitudes

We calculate electric-dipole reduced matrix elements using the form-independent third-order perturbation theory developed by Savukov and Johnson in Ref. [51]. Previously, a good precision of this method has been demonstrated for alkali-metal atoms. In this method, form-dependent "bare" amplitudes are replaced with form-independent random-phase approximation ("dressed") amplitudes to obtain form-independent third-order amplitudes to some degree of accu-

TABLE II. Reduced electric-dipole matrix elements in first, second, and third orders of perturbation theory in Yb II.

v	w	$Z_{vw}^{(DF)}$	$Z_{vw}^{(DF+2)}$	$Z_{vw}^{(DF+2+3)}$
$6s_{1/2}$	$6p_{1/2}$	3.2422	2.8523	2.6829
$6s_{1/2}$	$6p_{3/2}$	4.5426	4.0349	3.7676
$6p_{1/2}$	$7s_{1/2}$	2.2898	2.3512	2.2338
$6p_{3/2}$	$7s_{1/2}$	3.7574	3.8098	3.7042
$6s_{1/2}$	$7p_{1/2}$	0.0931	0.0794	−0.0686
$6s_{1/2}$	$7p_{3/2}$	0.3585	0.1187	0.1530
$5d_{3/2}$	$6p_{1/2}$	3.8610	3.4843	2.9709
$5d_{3/2}$	$6p_{3/2}$	1.6969	1.5555	1.3068
$5d_{5/2}$	$6p_{3/2}$	5.2001	4.7704	4.1204
$5d_{3/2}$	$7p_{1/2}$	0.2173	0.3780	0.0829
$5d_{3/2}$	$7p_{3/2}$	0.0239	0.0869	−0.0369
$5d_{5/2}$	$7p_{3/2}$	0.1114	0.2943	−0.0229
$6p_{1/2}$	$8s_{1/2}$	0.6087	0.6403	0.6158
$6p_{3/2}$	$8s_{1/2}$	0.9008	0.9274	0.8926
$7s_{1/2}$	$7p_{1/2}$	6.4633	6.3390	6.0500
$7s_{1/2}$	$7p_{3/2}$	8.9051	8.7506	8.3060
$7p_{1/2}$	$8s_{1/2}$	4.7636	4.8058	4.6452
$7p_{3/2}$	$8s_{1/2}$	7.6641	7.7019	7.5711
$6p_{1/2}$	$6d_{3/2}$	3.6652	3.6185	3.7094
$6p_{3/2}$	$6d_{3/2}$	1.8632	1.8264	1.8899
$6p_{3/2}$	$6d_{5/2}$	5.4672	5.3722	5.4787
$6d_{3/2}$	$7p_{1/2}$	9.3211	9.2209	8.6156
$6d_{3/2}$	$7p_{3/2}$	4.0898	4.0566	3.7603
$6d_{5/2}$	$7p_{3/2}$	12.4581	12.3474	11.5640

racy. As in the case of the third-order energy calculation, a limited number of partial waves with $l_{max} < 7$ is included. This restriction is not very important for ions considered here because third-order energy correction is smaller than the second-order energy correction but it gives rise to some loss of gauge invariance. The gauge independence serves as an additional check that no numerical problems occurred.

Length and velocity-form matrix elements from DF, second-order RPA, and third-order calculations are given in Table III for the limited number of transitions in Yb II. The $Z^{(DF)}$ values differ in L and V forms by 1%–5% for the $p-s$ and $s-p$ transitions except for the $6s-7p_j$ transitions with $L-V$ difference equal to 36% ($j=1/2$) and 16% ($j=3/2$). The largest $L-V$ difference (a factor of 100) is for the $5d_{3/2}-6p_{3/2}$ transitions. The $Z^{(DF)}$ values in L and V forms have different signs for this transition (see columns with the $Z^{(DF)}$ heading in Table III). The second-order RPA contribution completely removes this difference in $L-V$ values, and the L and V columns with the $Z^{(DF+2)}$ headings are almost identical. There are, however, small $L-V$ differences (0.01%–1%) in the third-order matrix elements. These remaining small differences can be explained by limitation in the number of partial waves taken into account in the evaluations of the third-order matrix elements.

C. Transition rates in Yb II ion

Wavelengths and transition rates A_r in Yb II calculated using third-order RMBPT are presented in Table IV. Two results of our RMBPT calculations are given in Table IV. The RMBPT[a] and RMBPT[b] values are evaluated using the $Z^{(DF+2+3)}$ values shown in the last columns of Tables II and III. Additionally, we presented the DF transition rate evaluated using the $Z^{(DF)}$ values. In all transition rate results given in columns with headings "DF," "RMBPT[a]," and "RMBPT[b]," we use recommended NIST energy values [36] shown in the third column of Table IV.

Two results of our RMBPT calculations given in Table IV are compared with available theoretical results presented by Migdalek [28], by Fawcett and Wilson [29], and by Biémont *et al.* [32]. The relativistic model potential approach which takes into account both valence-core electron exchange and correlation was used in Ref. [28]. In Ref. [29], the Slater integrals were first computed *ab initio* by a pseudorelativistic Hartree-Fock method and subsequently adjusted by means of a least-squares optimization routine which minimizes the discrepancies between observed and computed levels. The oscillator strengths and transition rates in Ref. [32] were calculated within the framework of a pseudorelativistic HFR approximation combined with a least-squares fitting of the calculated eigenvalues to the observed energy levels.

The pseudorelativistic Hartree-Fock method was used in Refs. [29,32]. One can see from Table IV that there is relatively small disagreement (about 10%–20%) between the values of Refs. [29,32] for most of transitions except for the $6s-7p_{3/2}$ transition (for which the results differ by a factor of 4). We already mentioned previously about the need for careful treatment of the RPA contribution for this transition. The values obtained by various approaches differed by a factor of two to ten for the $6s-7p_{3/2}$ transition as illustrated in Table IV. The best agreement (30%) for $6s-7p_{3/2}$ transition is found for A_r values calculated in DF approach and in Ref. [29] (1.72 [7] and 2.06 [7], respectively). Both RMBPT values for the $6s-6p$, $6p-7s$, $6p-8s$, $7s-7p$, $7p-8s$, and $6p-6d$ transitions are in better agreement with values from Ref. [28] (1%–10%) than from Ref. [29] (20%–50%). However, there is large disagreement (by a factor of 2) between our RMBPT values and values from Ref. [28] for the $6p-7d$ transitions while the difference between our RMBPT values and values from Ref. [29] are still 10%–30%.

D. Lifetimes values of the $6p_{1/2}$ and $6p_{3/2}$ levels in Yb II

If we were to evaluate the lifetimes using A_r values presented in Table IV, the results would be complete only for the $6p_{1/2}$ and $6p_{3/2}$ levels. Core excited states have to be considered to evaluate lifetimes for any other states except lowest-lying metastable state $5d_{3/2}$ (see, for example, [32]). Only two transitions ($6s-6p_{1/2}$ and $5d_{3/2}-6p_{1/2}$) contribute to the lifetime value of the $6p_{1/2}$ state and the three transitions ($6s-6p_{3/2}$, $5d_{3/2}-6p_{3/2}$, and $5d_{5/2}-6p_{3/2}$) contribute to the lifetime value of the $6p_{3/2}$ state. We see from Table IV that the main contributions to the lifetime of these states (99%) come from the $6s-6p_{1/2}$ and $6s-6p_{3/2}$ transitions, respectively.

TABLE III. Reduced electric-dipole matrix elements in first, second, and third orders of perturbation theory, calculated in lengths (L) and velocity (V) forms for Yb II.

Transitions		$Z_{vw}^{(DF)}$		$Z_{vw}^{(DF+2)}$		$Z_{vw}^{(DF+2+3)}$	
v	w	L	V	L	V	L	V
$6s_{1/2}$	$6p_{1/2}$	3.24219	3.09818	2.90971	2.90969	2.73086	2.73061
$6s_{1/2}$	$6p_{3/2}$	4.54262	4.32196	4.09664	4.09663	3.84463	3.84470
$6p_{1/2}$	$7s_{1/2}$	2.28979	2.21188	2.33357	2.33357	2.23722	2.23710
$6p_{3/2}$	$7s_{1/2}$	3.75738	3.60859	3.79276	3.79277	3.69969	3.69970
$6s_{1/2}$	$7p_{1/2}$	0.09310	0.05951	−0.15307	−0.15309	−0.13548	−0.13556
$6s_{1/2}$	$7p_{3/2}$	0.35850	0.30004	0.01547	0.01545	0.04391	0.04392
$5d_{3/2}$	$6p_{1/2}$	3.86104	−23.75603	3.53777	3.53901	3.78152	3.78485
$5d_{3/2}$	$6p_{3/2}$	1.69693	0.01089	1.57128	1.57130	1.54635	1.54676
$5d_{5/2}$	$6p_{3/2}$	5.20010	−1.16778	4.83048	4.83070	4.76905	4.76867
$5d_{3/2}$	$7p_{1/2}$	−0.21733	0.42044	0.35356	0.35356	0.11772	0.11744
$5d_{3/2}$	$7p_{3/2}$	0.02387	0.11556	0.07892	0.07892	−0.02271	−0.02279
$5d_{5/2}$	$7p_{3/2}$	0.11135	0.41060	0.26362	0.26361	0.00546	0.00540
$6p_{1/2}$	$8s_{1/2}$	0.60871	0.57935	0.64098	0.64098	0.62161	0.62157
$6p_{3/2}$	$8s_{1/2}$	0.90080	0.84792	0.91960	0.91960	0.88985	0.88985
$7s_{1/2}$	$7p_{1/2}$	6.46334	6.34152	6.35700	6.35700	6.07926	6.07904
$7s_{1/2}$	$7p_{3/2}$	8.90511	8.71579	8.77009	8.77010	8.35685	8.35689
$7p_{1/2}$	$8s_{1/2}$	4.76352	4.69088	4.79035	4.79035	4.65066	4.65053
$7p_{3/2}$	$8s_{1/2}$	7.66400	7.52174	7.68975	7.68976	7.57117	7.57119
$6p_{1/2}$	$6d_{3/2}$	3.66521	3.48364	3.62167	3.62168	3.67289	3.67297
$6p_{3/2}$	$6d_{3/2}$	1.86323	1.77354	1.83362	1.83362	1.87322	1.87318
$6p_{3/2}$	$6d_{5/2}$	5.46727	5.18187	5.38020	5.38021	5.43804	5.43808
$6d_{3/2}$	$7p_{1/2}$	9.32114	3.98198	9.22502	9.22533	8.94868	8.95086
$6d_{3/2}$	$7p_{3/2}$	4.08984	3.18605	4.05500	4.05502	3.86461	3.86453
$6d_{5/2}$	$7p_{3/2}$	12.45809	9.02019	12.35198	12.35213	11.82392	11.82408

Lifetimes (in ns) of $6p_{1/2}$ and $6p_{3/2}$ states in Yb II are presented in Table V. The RMBPT ($\tau^{(\mathrm{RMBPT}^a)}$ and $\tau^{(\mathrm{RMBPT}^b)}$) values are compared with theoretical (τ^{theor}) [5,29,32] and experimental data (τ^{expt}) [5–8,14,15,23]. There are very significant discrepancies between experimental measurements that are listed in Table V. The values of τ^{expt} range from 6.9 ± 0.6 [6] up to 8.10 ± 0.13 [15] for the $6p_{1/2}$ state, and from 5.5 ± 0.3 [8] up to 7.3 ± 0.5 [5] for the $6p_{3/2}$ state. Our RMBPT values are in better agreement with smallest values of τ^{expt} presented in Refs. [6,8] for the $6p_{1/2}$ and $6p_{3/2}$ states, respectively. In contrast, theoretical results τ^{th} given in Refs. [29,32] are in better agreement with largest values of τ^{expt} presented in Refs. [15,5] for the $6p_{1/2}$ and $6p_{3/2}$ states, respectively.

We already mentioned that the main contributions to the lifetime of the $6p_{1/2}$ and $6p_{3/2}$ states come from the $6s−6p_{1/2}$ and $6s−6p_{3/2}$ transitions. Using the A_r values for these transitions obtained by Migdalek [28] (values 1.46 [8] and 2.06 [8], last column of Table IV), we find the corresponding lifetimes to be 6.85 ns ($6p_{1/2}$ state) and 4.85 ns ($6p_{3/2}$ state) which is in excellent agreement with our RMBPT results. The many-body perturbation theory (MBPT) approximation was used in Ref. [14] to calculate the $6s−6p_{1/2}$ and $6s−6p_{3/2}$ matrix elements. Estimated lifetimes of the $6p_{1/2}$ and $6p_{3/2}$

state were equal to 7.0 and 5.0 ns, respectively [14]. Recently, relativistic coupled-cluster method was applied to compute the $6s−6p_{1/2}$ and $6s−6p_{3/2}$ matrix elements [35]. It yielded the values 2.781 and 3.914 a.u. for the $6s−6p_{1/2}$ and $6s−6p_{3/2}$ matrix elements, respectively. These results correspond to the 6.44 and 4.59 ns values for the lifetimes of the $6p_{1/2}$ and $6p_{3/2}$ states. These results are even smaller than our RMBPT lifetime values given in the first two lines of Table V.

IV. GROUND STATE STATIC POLARIZABILITIES FOR Yb II IONS

The calculation of the ground-state polarizabilities of Yb II ion provides another test of the quality of atomic-structure calculations and another measure of the size of correlation corrections. The static polarizability of Yb II ion is the sum of the polarizability of the ionic core α_c, a counter term α_{vc} compensating for excitation from the core to the valence shell which violates the Pauli principle, and a valence electron contribution α_v (see, for example, Refs. [52,53]),

$$\alpha = \alpha_c + \alpha_v + \alpha_{vc}. \tag{2}$$

We calculate α_c in the relativistic RPA approximation (see Johnson et al. [54] for details).

TABLE IV. Wavelengths $\lambda(\text{Å})$ and transition rates A_r (s^{-1}) for transitions in Yb II calculated using third-order RMBPT. We list third-order RMBPT results obtained using bare and dressed matrix elements in MBPT formulas in columns labeled RMBPT[a] and RMBPT[b], respectively. Our results are compared with theoretical values presented by Migdalek [28], by Fawcett and Wilson [29], and by Biémont *et al.* [32]. Numbers in brackets represent powers of ten.

Transitions		λ (Å)	Transition rates A_r (s^{-1})			Transition rates A_r (s^{-1})		
Lower	Upper	[[36]]	DF	RMBPT[a]	RMBPT[b]	[[29]]	[[32]]	[[28]]
$6s_{1/2}$	$6p_{1/2}$	3695.24	2.11[8]	1.45[8]	1.50[8]	1.14[8]	1.15[8]	1.46[8]
$6s_{1/2}$	$6p_{3/2}$	3290.31	2.93[8]	2.02[8]	2.10[8]	1.20[8]	1.36[8]	2.06[8]
$6p_{1/2}$	$7s_{1/2}$	3670.74	1.07[8]	1.02[8]	1.03[8]	8.34[7]	9.10[7]	9.45[7]
$6p_{3/2}$	$7s_{1/2}$	4181.99	1.96[8]	1.90[8]	1.90[8]	7.72[7]		1.76[8]
$6s_{1/2}$	$7p_{1/2}$	1569.70	2.27[6]	1.23[6]	4.81[6]	4.06[7]		2.04[6]
$6s_{1/2}$	$7p_{3/2}$	1557.85	1.72[7]	3.14[6]	2.58[5]	2.06[7]	7.55[6]	1.31[6]
$5d_{3/2}$	$6p_{1/2}$	24384.18	1.04[6]	6.17[5]	9.99[5]	7.18[5]	5.65[5]	
$5d_{3/2}$	$6p_{3/2}$	13456.36	5.99[5]	3.55[5]	4.97[5]	3.32[5]	2.87[5]	
$5d_{5/2}$	$6p_{3/2}$	16502.90	3.05[6]	1.91[6]	2.56[6]	1.74[6]	1.46[6]	
$5d_{3/2}$	$7p_{1/2}$	2454.26	3.24[6]	4.71[5]	9.50[5]	1.05[7]		
$5d_{3/2}$	$7p_{3/2}$	2425.35	2.02[4]	4.83[4]	1.83[4]	1.36[7]		
$5d_{5/2}$	$7p_{3/2}$	2508.83	3.98[5]	1.68[4]	9.55[2]	1.75[7]	1.93[7]	
$6p_{1/2}$	$8s_{1/2}$	2174.96	3.65[7]	3.73[7]	3.80[7]	5.99[7]		3.68[7]
$6p_{3/2}$	$8s_{1/2}$	2344.81	6.38[7]	6.26[7]	6.22[7]	7.70[7]		6.35[7]
$7s_{1/2}$	$7p_{1/2}$	10636.09	3.52[7]	3.08[7]	3.11[7]	2.47[7]		2.53[7]
$7s_{1/2}$	$7p_{3/2}$	10113.61	3.88[7]	3.38[7]	3.42[7]	2.11[7]		3.48[7]
$7p_{1/2}$	$8s_{1/2}$	10714.26	1.87[7]	1.78[7]	1.78[7]	1.82[7]		2.03[7]
$7p_{3/2}$	$8s_{1/2}$	11302.45	4.12[7]	4.02[7]	4.02[7]	2.02[7]		3.70[7]
$6p_{1/2}$	$6d_{3/2}$	2848.01	2.95[8]	3.02[8]	2.96[8]	2.21[8]		2.69[8]
$6p_{3/2}$	$6d_{3/2}$	3146.45	5.65[7]	5.81[7]	5.71[7]	2.43[7]		5.14[7]
$6p_{3/2}$	$6d_{5/2}$	3108.80	3.36[8]	3.37[8]	3.32[8]	1.29[8]		3.04[8]
$6d_{3/2}$	$7p_{1/2}$	65267.76	3.17[5]	2.70[5]	2.92[5]	2.31[5]		1.02[8]
$6d_{3/2}$	$7p_{3/2}$	49557.21	6.96[4]	5.88[4]	6.22[4]	3.73[4]		1.77[7]
$6d_{5/2}$	$7p_{3/2}$	61238.86	3.42[5]	2.95[5]	3.08[5]	1.78[5]		1.09[8]

With the $6s_{1/2}$ ground state, we obtain for α_v and α_{vc}

$$\alpha_v = \sum_{n=6}^{70} [I_v(np_{1/2}) + I_v(np_{3/2})], \qquad (3)$$

$$\alpha_{vc} = \sum_{n=2}^{5} [I_v(np_{1/2}) + I_v(np_{3/2})],$$

$$I_v(nlj) = \frac{2}{3(2j+1)} \frac{(Z_{v,nlj})^2}{E_{nlj} - E_v}. \qquad (4)$$

The calculation of the α_v is divided into two parts,

$$\alpha_v^{\text{main}} = \sum_{n=6}^{k} [I_v(np_{1/2}) + I_v(np_{3/2})],$$

$$\alpha_v^{\text{tail}} = \sum_{n=k+1}^{70} [I_v(np_{1/2}) + I_v(np_{3/2})]. \qquad (5)$$

We take k to be 12 in our calculations for Yb II. The values of α_v^{main} are calculated using RMBPT values of dipole matrix elements $Z_{v,nlj}$ (values $Z_L^{(\text{DF+2+3})}$ given in Table III) and experimental energies (or RMBPT energies, when we did not find experimental data). We use DF values to calculate α_v^{tail}. We use also DF values to calculate α_{vc} given by Eq. (3).

Our numerical results are given in Table VI. The main contribution comes from the first term $\alpha_v^{\text{main}}(6p)$, the second and third term $[\alpha_v^{\text{main}}(7p) + \alpha_v^{\text{main}}(8p)]$ contributions are equal to 1%, and all other ($n=9-12$) terms give only 0.1%. Static dipole polarizability of Yb$^+$ was calculated by Migdalek [28] using the core-polarization-corrected oscillator strengths. Three types of computation have been performed. In the first type (RMP), core polarization was completely neglected. The next two types include core polarization but differ in the value of the Yb^{2+} core polarizability (CP), which was equal to $7.36a_0^3$ and $11.14a_0^3$ for RMP+CPIa and RMP+CPIIb approximations, respectively. The core-polarization-corrected oscillator strength calculations produced the values equal to $54.48a_0^3$ (RMP+CPIa) and $48.18a_0^3$ (RMP+CPIb) for the valence dipole polarizability. Together with values of the Yb^{2+}

TABLE V. Lifetimes (in ns) of the $6p_{1/2}$ and $6p_{3/2}$ states in Yb II. The RMBPT ($\tau^{(\text{RMBPT}^a)}$) and ($\tau^{(\text{RMBPT}^b)}$) values are compared with theoretical (τ^{theor}) and experimental data (τ^{expt}).

	$6p_{1/2}$	$6p_{3/2}$
$\tau^{(\text{RMBPT}^a)}$	6.89	4.90
$\tau^{(\text{RMBPT}^b)}$	6.64	4.69
τ^{theor} [5]	7.0	5.0
τ^{theor} [29]	8.8	8.4
τ^{theor} [32]	8.60	7.23
τ^{expt} [5]	8.9 ± 0.5	7.3 ± 0.6
τ^{expt} [6]	6.9 ± 0.6	7.2 ± 0.8
τ^{expt} [7]		5.8 ± 0.6
τ^{expt} [8]	7.1 ± 0.4	5.5 ± 0.3
τ^{expt} [14]	8.0 ± 0.2	6.3 ± 0.3
τ^{expt} [15]	8.10 ± 0.13	
τ^{expt} [23]	8.07 ± 0.9	6.15 ± 0.09

core polarizability $7.36a_0^3$ (RMP+CPIa) and $11.14a_0^3$ (RMP+CPIb), the following values for the total static dipole polarizability of Yb$^+$ were obtained: $62.84a_0^3$ (RMP+CPIa) and $59.32a_0^3$ (RMP+CPIb). Our RMBPT value ($\alpha_v^{\text{RMBPT}}=62.04a_0^3$) is in a better agreement with the value in [28] obtained in the RMP+CPIa approximation. The Yb^{2+} core polarizability used in the RMP+CPIa approximation was equal to $7.36a_0^3$ that is in better agreement with our RPA value $\alpha_c=6.386a_0^3$ (see Table VI) than the value used in RMP+CPIb approximation [28].

V. HYPERFINE CONSTANTS FOR ^{171}Yb$^+$

Calculation of hyperfine constants follows the same pattern as the calculations of the reduced dipole matrix elements described in the previous section. The magnetic moments and nuclear spins used in present calculations are taken from [55]. In Table VII, we give the magnetic-dipole hyperfine constant A for ^{171}Yb II, and compare with available theoretical and experimental data from Refs. [13,16]. In this table,

TABLE VI. Contribution to the $6s_{1/2}$ static polarizability (a.u.) of Yb II.

$v=6s_{1/2}$	Contribution
$\alpha_v^{\text{main}}(6p)$	55.741
$\alpha_v^{\text{main}}(7p)$	0.021
$\alpha_v^{\text{main}}(8p)$	0.039
$\alpha_v^{\text{main}}(9p)$	0.05
$\alpha_v^{\text{main}}(10p)$	0.01
$\alpha_v^{\text{main}}(\text{total})$	55.815
α_v^{tail}	0.013
α_c^{RPA}	6.386
α_{vc}^{DF}	-0.177
$\alpha_v(\text{total})$	62.04

TABLE VII. Hyperfine constants A (in MHz) in ^{171}Yb$^+$ ($I=1/2$, $\mu=0.4919$ [55]). The DF and third-order data are compared with experimental measurements. and theoretical prediction [16].

v	$A^{(\text{DF})}$	$A^{(\text{DF}+2+3)}$	$A^{(\text{expt})}$	$A^{(\text{theor})}$
$6s_{1/2}$	9585	13172	12645(2) [a]	12730 [a]
$6p_{1/2}$	1544	2350	2104.9(1.3)[a]	2317[a]
$6p_{3/2}$	182.5	311.5	877(20)[b]	391[a]
$7s_{1/2}$	2885.4	3595.0		
$7p_{1/2}$	569.9	807.4		
$7p_{3/2}$	68.7	110.8		

[a]Reference [16].
[b]Reference [13].

we present the lowest-order $A^{(\text{DF})}$ and third-order $A^{(\text{DF}+2+3)}$ values for the $ns_{1/2}$, $np_{1/2}$, and $np_{3/2}$ levels with $n=6$ and 7. As discussed before for dipole matrix elements, third-order hyperfine constants $A^{(\text{DF}+2+3)}$ include RPA $A^{(\text{RPA})}$, Brueckner-orbital $A^{(\text{BO})}$, structural radiation $A^{(\text{SR})}$, and normalization $A^{(\text{NORM})}$ corrections. The differences between third-order and lowest-order results are 20–40% as illustrated in Table VII. The Brueckner-orbital term $A^{(\text{BO})}$ gives the largest correction for the $6s_{1/2}$, $6p_{1/2}$, and $7p_{1/2}$ levels; however, the RPA $A^{(\text{RPA})}$ term becomes larger than the $A^{(\text{BO})}$ term for the $7s_{1/2}$, $6p_{3/2}$, and $7p_{3/2}$ levels.

Our hyperfine constant values appear to be in better agreement with the theoretical values $A^{(\text{theor})}$ from Ref. [16] than with experimental data $A^{(\text{expt})}$ from the same Ref. [16]. The largest disagreement between the theoretical values ($A^{(\text{DF}+2+3)}$ and $A^{(\text{theor})}$ from Ref. [16]) and experimental measurement is found to be for the $6p_{3/2}$ level [13]. We see no explanation for this disagreement, as the correlation corrections do not appear to be significantly larger for this level than for the others.

Finally, we would like to demonstrate the dependence of the $A^{(\text{DF}+2+3)}(nlj)$ hyperfine constants on principal quantum number n. In Fig. 1, we present our $A^{(\text{DF}+2+3)}(nlj)$ values for the $ns_{1/2}$, $np_{1/2}$, and $np_{3/2}$ levels with $n=6-15$. One can see smooth n dependence of the $A^{(\text{DF}+2+3)}(nlj)$ values as additional check of our calculations.
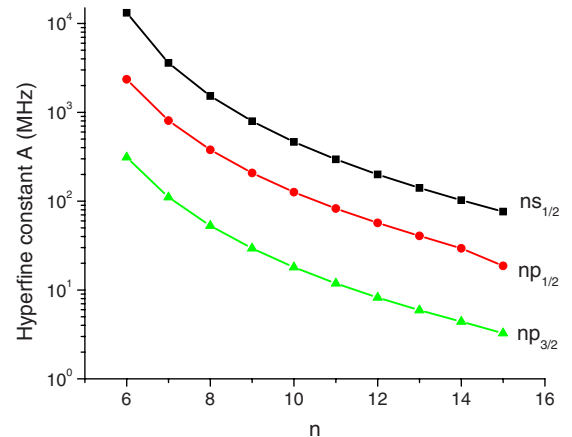
FIG. 1. (Color online) Hyperfine constants $A^{(\text{DF}+2+3)}(nlj)$ as function of n.

VI. HYPERFINE-INDUCED TRANSITION POLARIZABILITY OF THE ^{171}Yb II GROUND STATE

We now turn to the calculation of the quadratic Stark shift of the ground-state hyperfine interval ($F=1-F=0$) in ^{171}Yb II. The quadratic Stark shift is closely related to the black-body radiation shift discussed, for example, in Refs. [56,57] and our calculation follows the procedure outlined in [57].

The dominant second-order contribution to the polarizability difference between the two hyperfine components of the $6s$ state cancels and, therefore, the Stark shift of the hyperfine interval is governed by the third-order F-dependent polarizability $\alpha_F^{(3)}(0)$. The expression for the $\alpha_F^{(3)}(0)$ has been given in [56],

$$\alpha_F^{(3)}(0) = \frac{1}{3}\sqrt{(2I)(2I+1)(2I+2)}\begin{Bmatrix} j_v & I & F \\ I & j_v & 1 \end{Bmatrix}$$
$$\times g_I\mu_n(-1)^{F+I+j_v}(2T+C+R), \qquad (6)$$

where g_I is the nuclear gyromagnetic ratio, μ_n is the nuclear magneton equal to $0.4919\mu_B$ in ^{171}Yb II, $I=1/2$ is the nuclear spin, and $j_v=1/2$ is the total angular momentum of the atomic ground state. The F-independent sums for T, C, and R ($|v\rangle \equiv |6s_{1/2}\rangle$) are given by Eqs. (5)–(7) by Beloy *et al.* [56].

We note first that the values of T, C, and R in atomic units are

$$2T^{\mathrm{DF}} = 1.2333 \times 10^{-3}, \quad C^{\mathrm{DF}} = 2.2842 \times 10^{-5},$$

$$R^{\mathrm{DF}} = 1.9456 \times 10^{-3} \qquad (7)$$

in the DF approximation.

Since the value of C^{DF} is smaller than the T^{DF} and R^{DF} by two orders of magnitude, we did not recalculate the C term using the third-order RMBPT.

The expression for R is similar to the one for $\alpha^{E1}(0)$ [compare Eqs. (3) and (4) and expression for R in [56]]. The difference is an additional factor containing the diagonal hyperfine matrix element,

$$\langle 6s_{1/2}||T||6s_{1/2}\rangle^{(\mathrm{DF}+2+3)} = 2.4922 \times 10^{-6} \text{ a.u..}$$

We evaluate matrix elements $\langle v||rC_1||n\rangle$ in the third-order RMBPT approximation for $n \le 12$. We use recommended NIST energies [36] for $np=6p$ and $7p$, and the third-order RMBPT energies for $8 \le n \le 12$. The sum of the terms for $n \le 12$ is $R_{n\le 12} = 1.5096 \times 10^{-3}$. The remainder of the sum, evaluated in the DF approximation, $R_{n>12} = 4.3 \times 10^{-7}$, leads to $R^{(\mathrm{DF}+2+3)} = 1.5100 \times 10^{-3}$.

The expression for T includes sums over two indices m and n. To calculate the dominant part of T, we limit sum over m to six states ($m=6p_{1/2}$, $6p_{3/2}$, $7p_{1/2}$, and $7p_{3/2}$) and sum over n to $n \le 26$,

$$T_{n\le26}^{m\le7} = -\frac{1}{2}\sum_{ns=7s}^{26s}\frac{\langle ns||T^{(1)}||6s\rangle}{(E_{ns}-E_{6s})}$$

$$\times \left[\frac{\langle 6s||rC_1||6p_{1/2}\rangle\langle 6p_{1/2}||rC_1||ns\rangle}{(E_{6p_{1/2}}-E_{6s})} \right.$$

$$-\frac{\langle 6s||rC_1||6p_{3/2}\rangle\langle 6p_{3/2}||rC_1||ns\rangle}{(E_{6p_{3/2}}-E_{6s})}$$

$$+\frac{\langle 6s||rC_1||7p_{1/2}\rangle\langle 7p_{1/2}||rC_1||ns\rangle}{(E_{7p_{1/2}}-E_{6s})}$$

$$\left. -\frac{\langle 6s||rC_1||7p_{3/2}\rangle\langle 7p_{3/2}||rC_1||ns\rangle}{(E_{7p_{3/2}}-E_{6s})} \right]. \qquad (8)$$

The sum of the four contributions from Eq. (8) is 5.8098×10^{-4}. The ratio of contributions to the sum from the $6p$ and $7p$ states is equal to 50; therefore the sum over m converges very rapidly. The relatively small remainder $T - T_{n>26}^{m>7} = 0.0056 \times 10^{-4}$ is evaluated in the DF approximation, leading to a final value $T^{(\mathrm{DF}+2+3)} = 5.8154 \times 10^{-4}$. Combining these contributions, we obtain

$$2T^{\mathrm{DF}+2+3} + C^{\mathrm{DF}} + R^{\mathrm{DF}+2+3} = 2.6959 \times 10^{-3} \text{ a.u.} \qquad (9)$$

The F-dependent factor [see Eq. (6)],

$$A(F) = \frac{g_I\mu_n}{3}\sqrt{(2I)(2I+1)(2I+2)} \times \begin{Bmatrix} j_v & I & F \\ I & j_v & 1 \end{Bmatrix}(-1)^{F+I+j_v}$$

is equal to $-0.401\,635$ for $F=0$ and $0.133\,878$ for $F=1$. Using these values and the result from Eq. (9), we obtain

$$\Delta\alpha_{\mathrm{hf}} = [\alpha_{F=1}^{(3)}(0) - \alpha_{F=0}^{(3)}(0)] = 1.4437 \times 10^{-3} \text{ a.u.}$$

The Stark shift coefficient k defined as $\Delta\nu = kE^2$ is $k = -\frac{1}{2}[\alpha_{F=1}^{(3)}(0) - \alpha_{F=0}^{(3)}(0)]$. Converting from atomic units, we obtain

$$k^{(\mathrm{DF}+2+3)} = -7.2185 \times 10^{-4} \text{ a.u.}$$
$$= -1.7962 \times 10^{-11} \text{ Hz/(V/m)}^2.$$

In the DF approximation [Eq. (7)], we find $k^{(\mathrm{DF})} = -2.1332 \times 10^{-11}$ Hz/(V/m)^2.

The relative blackbody radiative shift β is defined as

$$\beta = -\frac{2}{15}\frac{1}{\nu_{\mathrm{hf}}}(\alpha\pi)^3T^4\Delta\alpha_{\mathrm{hf}}(6s_{1/2}), \qquad (10)$$

where ν_{hf} is the ^{171}Yb$^+$ hyperfine ($F=1$ and $F=0$) splitting equal to 12 645 MHz and T is a temperature taken to be 300 K. Using those factors, we can rewrite Eq. (10) as

$$\beta = -6.810 \times 10^{-13}\Delta\alpha_{\mathrm{hf}}(6s_{1/2}). \qquad (11)$$

Using the value for $\Delta\alpha_{\mathrm{hf}}(6s_{1/2}) = 1.4437 \times 10^{-3}$ a.u., we obtain finally

$$\beta^{(\mathrm{DF}+2+3)} = -0.983 \times 10^{-15}. \qquad (12)$$

In Table VIII, we compare our results for the Stark shift coefficient k and the relative blackbody radiative shift β with theoretical calculations from Ref. [2]. Our results and those

TABLE VIII. The Stark shift coefficient k in 10^{-10} Hz/(V/m)^2 and the relative blackbody radiative shift β in 10^{-14}. Comparison with theoretical calculations from Ref. [2].

	k	β
Present	−0.1796	−0.0983
Ref. [2]	−0.171(9)	−0.094(5)

of [2] are obtained using *ab initio* approaches. In both calculations, the RMBPT method was used; however, different methods were used to calculate matrix elements. Good agreement of both results should be useful for future experiments.

VII. CONCLUSION

In summary, a systematic RMBPT study of the energies of the $ns_{1/2}$, np_j, nd_j, and nf_j ($n \leq 8$) states in singly ionized ytterbium is presented. The energy values are in good agree-ment with existing experimental data. A systematic relativistic MBPT study of reduced matrix elements and transition rates for electric-dipole transitions which includes the $6s$, $7s$, $8s$, $6p$, $7p$, $5d$, and $6d$ states is conducted. Lifetime values are determined for the $6p$ states. Electric-dipole ($6s_{1/2} - np_j$, $n = 6-12$) matrix elements are calculated to obtain the ground-state E1 polarizabilities. All of the above-mentioned matrix elements are determined using the third-order RMBPT method. Hyperfine A values are presented for the first low-lying levels up to $n = 7$. The quadratic Stark shift of the ground-state hyperfine interval in ^{171}Yb II is also evaluated and compared with other available results.

ACKNOWLEDGMENTS

[1] S. Olmschenk, K. C. Younge, D. L. Moehring, D. N. Matsukevich, P. Maunz, and C. Monroe, Phys. Rev. A **76**, 052314 (2007).

[2] E. J. Angstmann, V. A. Dzuba, and V. V. Flambaum, Phys. Rev. A **74**, 023405 (2006).

[3] Chr. Tamm, B. Lipphardt, H. Schnatz, R. Wynands, S. Weyers, T. Schneider, and E. Peik, IEEE Trans. Instrum. Meas. **56**, 601 (2007).

[4] S. J. Adelman, Astrophys. J., Suppl. **27**, 183 (1974).

[5] M. L. Burshtein, Ya. F. Verolainen, V. A. Komarovskii, A. L. Osherovich, and N. P. Penkin, Opt. Spectrosc. **37**, 351 (1974).

[6] T. Andersen, O. Poulsen, P. S. Ramanujam, and A. Petrakiev Petkov, Sol. Phys. **44**, 257 (1975).

[7] F. H. K. Rambow and L. D. Schearer, Phys. Rev. A **14**, 738 (1976).

[8] K. B. Blagoev, V. A. Komarovskii, and N. P. Penkin, Opt. Spectrosc. **45**, 832 (1978).

[9] R. Blatt, H. Schnatz, and G. Werth, Phys. Rev. Lett. **48**, 1601 (1982).

[10] R. Blatt, H. Schnatz, and G. Werth, Z. Phys. A **312**, 143 (1983).

[11] A. Munch, M. Berkler, Ch. Gerz, D. Wilsdorf, and G. Werth, Phys. Rev. A **35**, 4147 (1987).

[12] H. Lehmitz, J. Hattendorf-Ledwoch, R. Blatt, and H. Harde, Phys. Rev. Lett. **62**, 2108 (1989).

[13] R. W. Berends and L. Maleki, J. Opt. Soc. Am. B **9**, 332 (1992).

[14] R. M. Lowe, P. Hannaford, and A.-M. Martensson-Pendrill, Z. Phys. D: At., Mol. Clusters **28**, 283 (1993).

[15] R. W. Berends, E. H. Pinnington, B. Guo, and Q. Ji, J. Phys. B **26**, L701 (1993).

[16] A.-M. Martensson-Pendrill, D. S. Gough, and P. Hannaford, Phys. Rev. A **49**, 3351 (1994).

[17] E. H. Pinnington, R. W. Berends, and Q. Ji, Phys. Rev. A **50**, 2758 (1994).

[18] D. J. Seidel and L. Maleki, Proceedings of the 1994 IEEE International Frequency Control Symposium (unpublished), Catalog No. 94CH3446-2, p. 761.

[19] K. B. Blagoev and V. A. Komarovskii, At. Data Nucl. Data Tables **56**, 1 (1994).

[20] R. C. Zhao, W. Huang, X. Y. Xu, X. M. Tong, Y. Z. Qu, C. B. Xu, and P. Xue, Phys. Rev. A **53**, 3994 (1996).

[21] P. Taylor, M. Roberts, S. V. Gateva-Kostova, R. B. M. Clarke, G. P. Barwood, W. R. C. Rowley, and P. Gill, Phys. Rev. A **56**, 2699 (1997).

[22] M. Roberts, P. Taylor, G. P. Barwood, P. Gill, H. A. Klein, and W. R. C. Rowley, Phys. Rev. Lett. **78**, 1876 (1997).

[23] E. H. Pinnington, G. Rieger, and J. A. Kernahan, Phys. Rev. A **56**, 2421 (1997).

[24] Z. S. Li, S. Svanberg, P. Quinet, X. Tordoir, and E. Biémont, J. Phys. B **32**, 1731 (1999).

[25] N. Yu and L. Maleki, Phys. Rev. A **61**, 022507 (2000).

[26] E. Biémont, P. Quinet, Zhenwen Dai, Jiang Zhankui, Zhang Zhiguo, Huailiang Xu, and S. Svanberg, J. Phys. B **35**, 4743 (2002).

[27] E. Biémont and P. Quinet, Phys. Scr. **T105**, 38 (2003).

[28] J. Migdalek, J. Quant. Spectrosc. Radiat. Transf. **28**, 61 (1982).

[29] B. C. Fawcett and M. Wilson, At. Data Nucl. Data Tables **47**, 241 (1991).

[30] K. Koc and J. Migdalek, J. Phys. B **25**, 907 (1992).

[31] E. Eliav, U. Kaldor, and Y. Ishikawa, Phys. Rev. A **52**, 291 (1995).

[32] E. Biémont, J.-F. Dutrieux, I. Martin, and P. Quinet, J. Phys. B **31**, 3321 (1998).

[33] E. Biémont and P. Quinet, Phys. Rev. Lett. **81**, 3345 (1998).

[34] V. A. Dzuba, V. V. Flambaum, and M. V. Marchenko, Phys. Rev. A **68**, 022506 (2003).

[35] M. K. Nayak and R. K. Chaudhuria, Eur. Phys. J. D **37**, 171 (2006).

[36] Yu. Ralchenko, F.-C. Jou, D. E. Kelleher, A. E. Kramida, A. Musgrove, J. Reader, W. L. Wiese, and K. Olsen, NIST Atomic Spectra Database, version 3.0.2; http://physics.nist.gov/asd3

[37] W. R. Johnson, S. A. Blundell, and J. Sapirstein, Phys. Rev. A **37**, 2764 (1988).

[38] U. I. Safronova, I. M. Savukov, M. S. Safronova, and W. R. Johnson, Phys. Rev. A **68**, 062505 (2003).

[39] I. M. Savukov, W. R. Johnson, U. I. Safronova, and M. S. Safronova, Phys. Rev. A **67**, 042504 (2003).

[40] U. I. Safronova and W. R. Johnson, Phys. Rev. A **69**, 052511 (2004).

[41] L. W. Fullerton and G. A. Rinker, Jr., Phys. Rev. A **13**, 1283 (1976).

[42] P. J. Mohr, Ann. Phys. (N.Y.) **88**, 26 (1974).

[43] P. J. Mohr, Ann. Phys. (N.Y.) **88**, 52 (1974).

[44] P. J. Mohr, Phys. Rev. Lett. **34**, 1050 (1975).

[45] S. A. Blundell, W. R. Johnson, M. S. Safronova, and U. I. Safronova, Phys. Rev. A **77**, 032507 (2008).

[46] S. A. Blundell, Phys. Rev. A **47**, 1790 (1993).

[47] M. H. Chen, K. T. Cheng, W. R. Johnson, and J. Sapirstein, Phys. Rev. A **74**, 042510 (2006).

[48] W. R. Johnson, S. A. Blundell, and J. Sapirstein, Phys. Rev. A **37**, 307 (1988).

[49] W. R. Johnon, Z. W. Liu, and J. Sapirstein, At. Data Nucl. Data Tables **64**, 279 (1996).

[50] U. I. Safronova, M. S. Safronova, and W. R. Johnson, Phys. Rev. A **71**, 052506 (2005).

[51] I. M. Savukov and W. R. Johnson, Phys. Rev. A **62**, 052512 (2000).

[52] T. R. Fowler and J. Yellin, Phys. Rev. A **1**, 1006 (1970).

[53] M. S. Safronova and C. W. Clark, Phys. Rev. A **69**, 040501(R) (2004).

[54] W. R. Johnson, D. Kolb, and K. N. Huang, At. Data Nucl. Data Tables **28**, 333 (1983).

[55] http://www.webelements.com

[56] K. Beloy, U. I. Safronova, and A. Derevianko, Phys. Rev. Lett. **97**, 040801 (2006).

[57] W. R. Johnson, U. I. Safronova, A. Derevianko, and M. S. Safronova, Phys. Rev. A **77**, 022510 (2008).